



Non-isothermal Crystallization Kinetics and Nucleation Activity of Filler in Polypropylene/Microcrystalline Cellulose Composites

Xiu Ling Zhu, Chao Sheng Wang, Biao Wang, and Hua Ping Wang*

State Key Laboratory for Modification of Chemical Fiber and Polymer Materials
College of Materials Science and Engineering, Donghua University
Shanghai-201620, P. R. China

Received 20 December 2007; accepted 16 March 2008

ABSTRACT

The non-isothermal crystallization kinetics of isotactic polypropylene (iPP) and iPP/microcrystalline cellulose 1 (MCC1) (hydrolyzed by HCl) and iPP/microcrystalline cellulose 2 (MCC2) (hydrolyzed by H₂SO₄) composites were investigated by differential scanning calorimetry technique (DSC) with various cooling rates. The Avrami, Ozawa, and Mo equations were applied to describe the non-isothermal crystallization kinetics and to determine the crystallization parameters of the composites. The results show that the values of $t_{1/2}$ for iPP/MCCs composites are lower than that for iPP. The value of $F(T)$ systematically increases with increasing relative degree of crystallinity. Non-isothermal crystallizations of iPP/MCCs composites correspond to three-dimensional growth with heterogeneous nucleation and MCCs acted as nucleating agent in iPP matrix. The addition of microcrystalline cellulose has greatly reduced the spherulitic size of iPP.

Key Words:

polypropylene;
microcrystalline cellulose;
non-isothermal crystallization;
nucleating agent;
spherulite size.

INTRODUCTION

Isotactic polypropylene (iPP) is a semicrystalline thermoplastic polymeric material that has been widely used because of its attractive combination of good processability, good mechanical properties, and good chemical resistance. However, inadequate stiffness and high brittleness of iPP have limited its versatile application to some extent. Compounding with inor-

ganic/organic particles is a simple, effective, and economical method to improve the mechanical and thermal properties of iPP. In recent years some studies on the structure and property of inorganic/organic particles-filled polymer blends have been conducted [1-7]. It is found that usually by addition of inorganic/organic particles to iPP there is a slight increase in the

(*) To whom correspondence to be addressed.

E-mail: wanghp@dhu.edu.cn

crystallization temperatures of iPP while the crystallization rate is accelerated and finally the degree of crystallinity is increased as well. It has been reported that 0.8 wt% of an organic phosphorus particles added to iPP increases the nucleation density by six orders of magnitude and the crystallization temperature by 12 K [8].

Microcrystalline cellulose (MCC) whose amorphous regions are removed by acid hydrolysis can be a very promising cellulosic reinforcement for polymers. Basically it is crystalline cellulose derived from high quality wood pulp and it is expected to disintegrate into cellulose whiskers after being completely hydrolyzed. Native cellulose is one of the strongest and stiffest natural fibres available; with estimated theoretical modulus of 167.5 GPa [9] it has a high potential to act as reinforcing agent in polymers [10-15]. This cellulose fibril can be about 5-10 nm in diameter and the length varies from 100 nm to several micrometers. MCC [16] has the advantage of having high specific surface area compared to the other conventional cellulose fibres.

In this article, we investigate the effect of nucleation of MCC hydrolyzed by different acids on the non-isothermal crystallization kinetics of iPP/MCC composites. Several non-isothermal crystallization kinetic equations were employed to deal with the non-isothermal crystallization data. The kinetic parameters like the Avrami exponent was evaluated from the data based on differential scanning calorimetry (DSC) crystallization exotherms for iPP and iPP/MCC composites. Furthermore, polarized optical microscopy technique was used to display the effect of MCC on the nucleation density of iPP.

EXPERIMENTAL

Materials

Isotactic polypropylene (S 950) used in the study was purchased from Sinopec Yangzi Petrochemical Co. Ltd., with the melt index 26.0 g/10 min; density 905 kg/m³. Microcrystalline cellulose 1 (MCC1) was hydrolyzed by HCl (3 mol/L, 30 min, 102°C). Microcrystalline cellulose 2 (MCC2) was hydrolyzed by H₂SO₄ (1.5 mol/L, 30 min, 102°C) [17]. Both MCC1 and MCC2 were made in our laboratory with

5-50 μm in length and about 20 μm in diameter (cellulose I type).

Preparation of Composites

Samples of iPP, MCC1, and MCC2 were dried in vacuo at 60°C for 10 h. MCCs were pretreated at first and then mixed with iPP, separately. Composites were prepared by melt-mixing method with a mini-type extrusion machine (DACA, American). The mixing was carried out at 195°C at 75 rpm for 5 min. The ratios of MCC1 or MCC2 to iPP were 1%, 2%, and 3% and each resultant composite is abbreviated as (A: MCC1) A-1, A-2, and A-3 or (S: MCC2) S-1, S-2, and S-3.

Differential Scanning Calorimetry

Differential scanning calorimetry (DSC 822e, Mettler-Toledo, Switzerland) was employed to study the crystallization behaviours of the composites. About 5.0 mg samples were used. Indium was used for temperature calibration ($T_m = 156.6^\circ\text{C}$, $\Delta H_m = 28.4 \text{ J/g}$). Samples were heated at a rate of 10 K/min to 473 K for 5 min to erase the thermal history effects and then cooled to 323 K at various rates of 5.0, 7.5, 10.0, 12.5, 15.0 K/min. Finally the DSC cooling scanning curves were recorded. All the measurements were carried out under a nitrogen atmosphere to prevent extensive thermal degradation.

Polarized Optical Microscopy

The spherulite morphology and growth of iPP/MMC composite was observed with an Olympus BX51 polarized light optical microscope (POM) equipped with crossed polars and a hot stage (Linkam THMS 600). The samples were hot pressed into films of thickness 0.02 mm. After that, the film sample was heated to 473 K for 1 min via the hot stage and then cooled to the desired crystallization temperature (T_c) where, the spherulitic growth was monitored. Micrographs were taken at various time periods for measuring the spherulite radii (R).

RESULTS AND DISCUSSION

Crystallization Behaviour

Figures 1a-1f and Table 1 show that the higher the

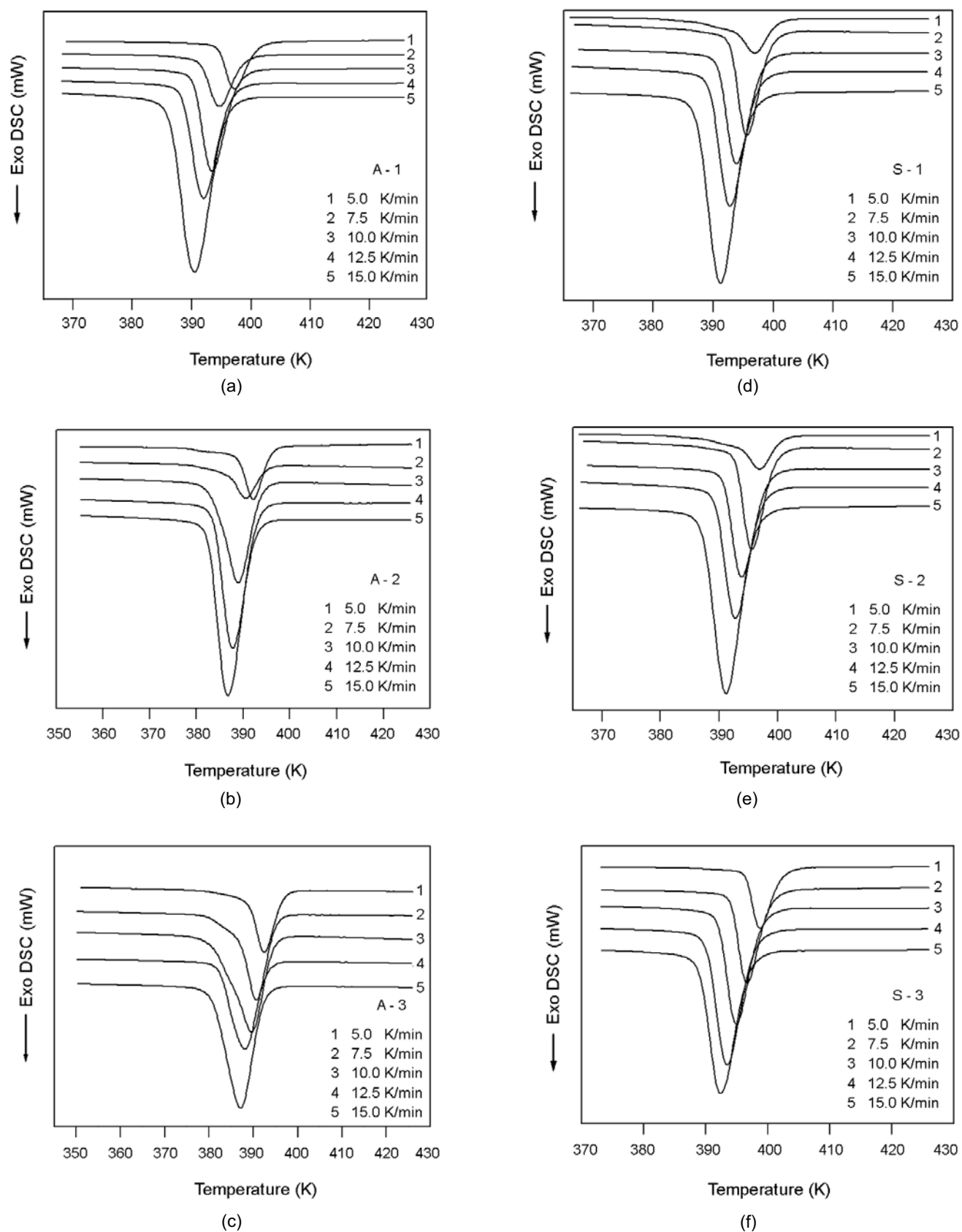


Figure 1. DSC Thermograms of: (a) A-1, (b) A-2, (c) A-3, (d) S-1, (e) S-2, and (f) S-3 composites during non-isothermal crystallization at different cooling rates.

Table 1. Values of the T_p at various cooling rates.

R (K/min)	T_p (K)						
	PP	A-1	A-2	A-3	S-1	S-2	S-3
5.0	389.9	391.6	392.2	392.4	397.2	396.9	398.8
7.5	388.3	389.2	390.5	390.7	394.7	395.5	396.7
10.0	386.9	387.6	388.9	389.6	393.4	393.8	394.9
12.5	385.3	386.4	387.6	388.0	392.0	392.8	393.5
15.0	384.1	385.4	386.6	386.9	390.4	391.1	392.4

cooling rate, the shorter time would be needed for completion of crystallization. It is shown that obviously both MCC1 and MCC2 enhance the crystallization peak temperature (T_p). MCC2 seems to be more effective than MCC1.

To obtain some information about the crystallization kinetics, the data in Figures 1a-1f were transformed to the relationship-of relative degree of crystallization versus time and macromechanics model was used to analyze the data. The relationship of the relative degree of crystallization versus time is shown in Figures 2a-2f. It can be seen that the higher the cooling rate, the shorter the time for completion of the crystallization is needed.

The half-time of non-isothermal crystallization, $t_{1/2}$ could be obtained from Figures 2a-2f for iPP and iPP/MCCs composites and the results are listed in Table 2. As expected, the value of $t_{1/2}$ decreases with the increasing of cooling rates of iPP and iPP/MCCs composites. Moreover, at a given cooling rate, the values of $t_{1/2}$ for iPP/MCCs composites are lower than those for iPP, signifying that the addition of MCCs can accelerate the overall crystallization process. It appears that MCC2 is more effective than MCC1.

Non-isothermal Crystallization Kinetics

Isothermal crystallization kinetics was analyzed using the Avrami theories [18,19] while, the non-isothermal crystallization kinetics was more complicated. The crystallization rate and mechanism can be influenced by many factors: not only the crystallization temperature and molecular weight, but also the molecular orientation, thermal history, and the presence of additives. In this paper, we used the Jeziorny's [20], Ozawa's [21] and Mo's analyses [22]

to investigate the non-isothermal crystallization kinetics of iPP/MMCs composites.

Jeziorny Analysis

This analysis is based on Avrami equation. Supposing the temperature is not changed when crystallization is progressing, then the non-isothermal crystallization process could be calculated as:

$$X_t = 1 - \exp(-k_t t^n) \quad (1)$$

where, X_t is the relative degree of crystallinity which is defined as:

$$X_t = \frac{\int_{T_0}^T (dH_c / dT) dT}{\int_{T_0}^{T_\infty} (dH_c / dT) dT} \quad (2)$$

where, T_0 and T_∞ are the temperatures at which crystallization starts and stops, and k_t and n denote the nucleation and growth rate constant and the Avrami exponent, respectively. It is known that the value of n strongly depends on the mechanism of nucleation and the morphology of crystal growth. The ideal n must be an integer whose value is usually between 1 and 4. For polymers, n will not always be an integer, because of the existence of homogeneous nucleation, heterogeneous nucleation, the second crystallization, etc. The Avrami crystallization constant, k_t , is related to the nucleation and crystallization rates. Taking the double logarithmic form of eqn (1) gives:

$$\ln[-\ln(1 - X_t)] = \ln k_t + n \ln t \quad (3)$$

Thus, the values of k_t and n can be obtained from the intercepts and slopes of the linear plots of $\ln[-\ln(1 -$

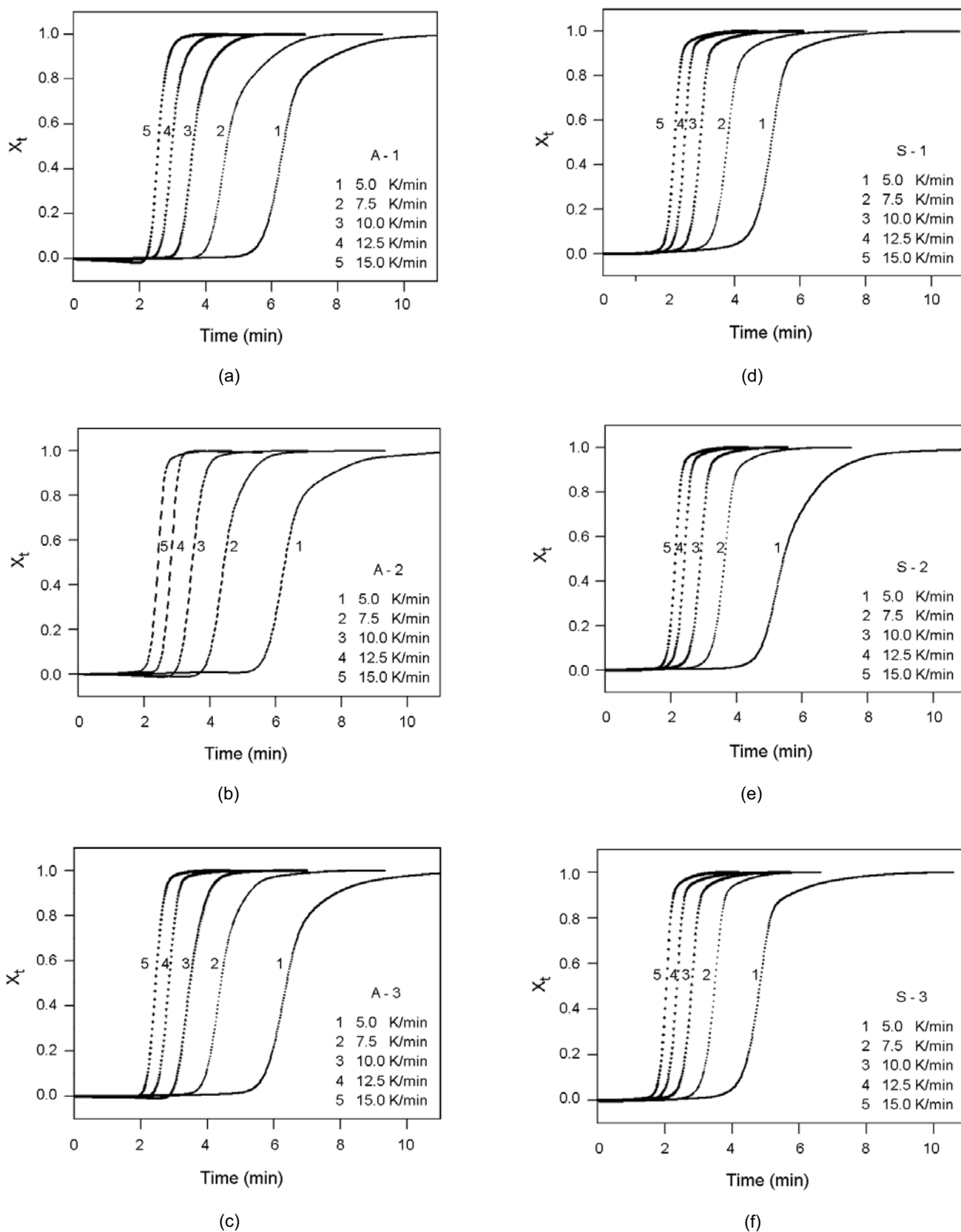


Figure 2. Relative crystallinity degree versus time for non-isothermal crystallization of: (a) A-1, (b) A-2, (c) A-3, (d) S-1, (e) S-2, and (f) S-3 composites at various cooling rates.

Table 2. Values of $t_{1/2}$ at various cooling rates.

R (K/min)	$t_{1/2}$						
	PP	A-1	A-2	A-3	S-1	S-2	S-3
5.0	6.9	6.4	6.37	6.32	5.06	5.39	4.85
7.5	5.41	4.64	4.5	4.41	3.85	3.69	3.53
10.0	4.35	3.69	3.5	3.46	2.99	2.89	2.78
12.5	4.10	3.02	2.91	2.8	2.52	2.44	2.36
15.0	3.64	2.58	2.51	2.43	2.15	2.07	1.99

X_t] versus $\ln t$, respectively (Figure 3). Then, the modified equation for the non-isothermal crystallization process is:

$$\ln k_c = \ln k_t / R \quad (4)$$

where, k_c and R are the polymeric non-isothermal crystallization parameter and the cooling rate, respectively.

As shown in Figure 3, there is a good linear relationship between $\ln[-\ln(1-X_t)]$ and $\ln t$ for iPP/MCCs composites. Non-isothermal crystallization parameter may be calculated from the results of Figure 3 and eqns (3) and (4) (Table 3). For the same sample, k_c rises with the cooling rate, indicating a faster crystallization rate. Both MCC1 and MCC2 could elevate the crystallization rate of iPP when the cooling rates are being equal. Taking the cooling rate of 5 K/min, for example, the exponent n for A-1, A-2, and A-3 varies from 4.35 to 3.87 and from 4.56 to 3.26 for S-1, S-2, and S-3. The decrease of n values with increasing amount of MCC means that the heterogeneous nucleation becomes more obvious and the MCC acted as a nucleating agent in iPP matrix. The n values also indicate that non-isothermal crystallizations of iPP/MCCs composites correspond to tri-dimensional growth. The degree of hydrolysis for MCC2 which has been hydrolyzed by H_2SO_4 is higher than that of MCC1 hydrolyzed by HCl. The interaction between MCC2 and iPP matrix may be stronger than that between MCC1 and iPP matrix. The n values of MCC2 are lower than those of MCC1 and oppositely the k_c values of MCC2 are higher than those of MCC1 at the same cooling rate. Therefore, the heterogeneous nucleation effect of MCC2 must be stronger than that of MCC1.

Ozawa Analysis

The alternative approach adopted here is the Ozawa equation [21].

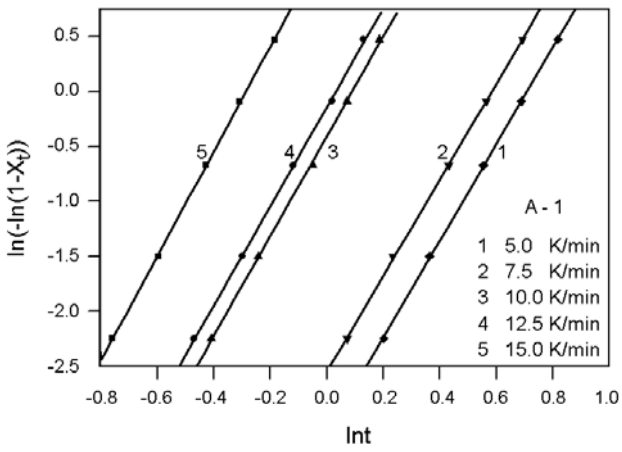
$$1-X_t = \exp[-K(T)/R^m] \quad (5)$$

where, $K(T)$ is a cooling function and m is the Ozawa exponent that depends on the dimension of crystal growth. Taking the double-logarithmic form eqn (5) gives:

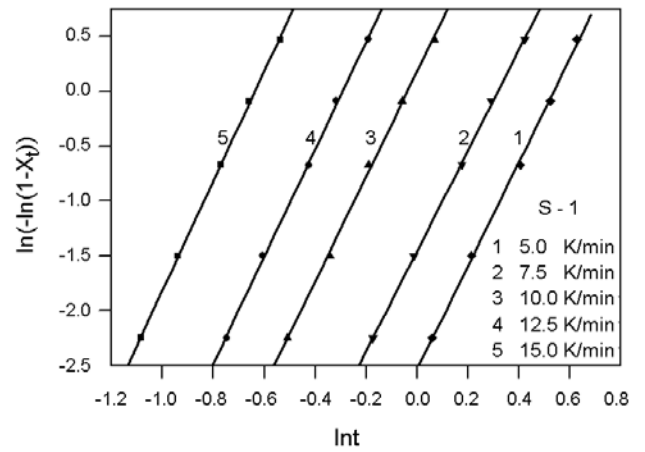
$$\ln[-\ln(1-X_t)] = \ln K(T) + m \ln R \quad (6)$$

Studying the process at different cooling rates and plotting $\ln[-\ln(1-X_t)]$ against $\ln R$ at a given temperature, a straight line should be obtained if the Ozawa method is valid. Then, the parameters of m and $K(T)$ can be determined from the slope and intercept, respectively.

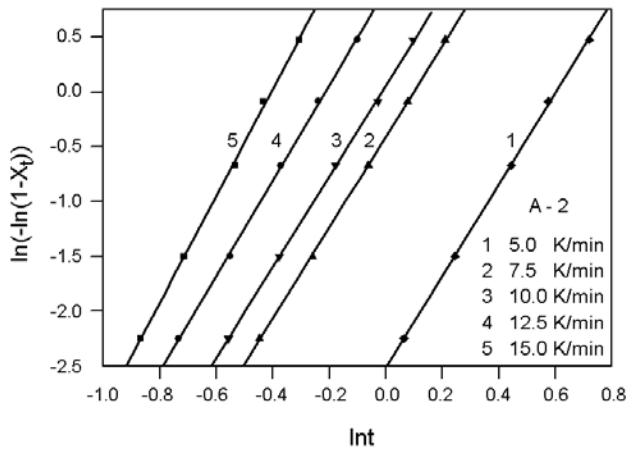
The results based on Ozawa method are shown in Figure 4. It is clearly seen that the curves in the plots of $\ln[-\ln(1-X_t)]$ vs. $\ln R$ for A-1 and S-1 do not exhibit a linear relationship. This might be reasonable, because the upper parts are related with the later stages during which crystallization is retarded, as it takes place in a constrained environment. Ozawa, in his approach, ignored the secondary crystallization and the dependence of the folded length on temperature [23]. Lopez et al. [24] claimed that during cooling, secondary crystallization could not take place due to the continuous decrease in temperature. However, it is known that Ozawa analysis cannot describe adequately the crystallization kinetics of polymers such as PE, PEEK, and nylon-11[25] for which a large part of crystallinity is attributed to secondary crystallization [26]. Thus, in iPP/MMCs composites of the



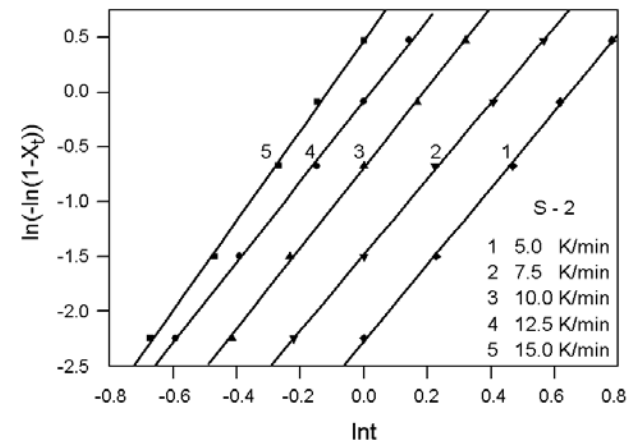
(a)



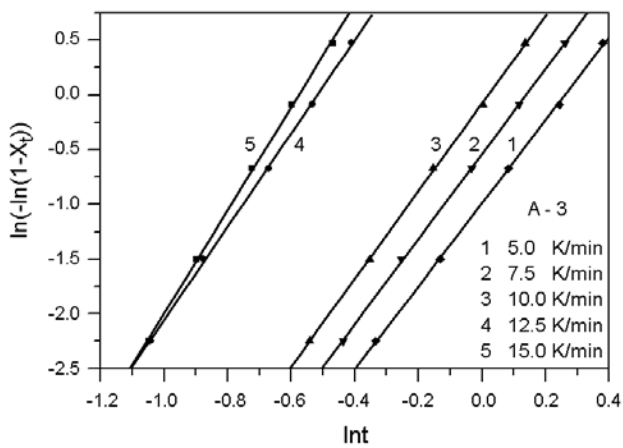
(d)



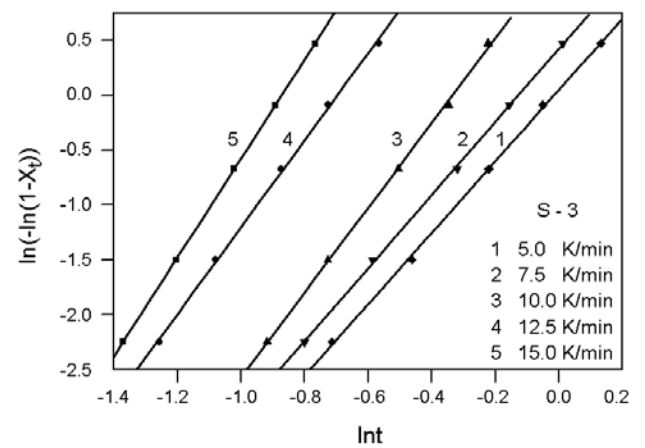
(b)



(e)



(c)



(f)

Figure 3. Plots of $\ln(-\ln(1-X_t))$ versus $\ln t$ for crystallization of: (a) A-1, (b) A-2, (c) A-3, (d) S-1, (e) S-2, and (f) S-3 composites.

Table 3. Values of the n , k_c and $\ln k_t$ at various cooling rates.

Sample	R (K/min)	n	k_c	$\ln k_t$
PP	5.0	4.01	0.54	-3.0809
	7.5	4.15	0.71	-2.5688
	10.0	4.22	0.96	-0.4082
	12.5	4.37	0.99	-0.1256
	15.0	4.39	1.1	1.4296
A-1	5.0	4.35	0.54	-3.0809
	7.5	4.40	0.71	-2.5687
	10.0	4.50	0.96	-0.4082
	12.5	4.61	0.99	-0.1256
	15.0	4.91	1.1	1.4297
A-2	5.0	4.15	0.61	-2.4715
	7.5	4.17	0.82	0.0746
	10.0	4.21	0.96	-0.4082
	12.5	4.38	1.08	0.9620
	15.0	4.85	1.14	1.9654
A-3	5.0	3.87	0.82	-0.9923
	7.5	3.91	0.93	-0.5443
	10.0	3.96	0.99	-0.1005
	12.5	4.24	1.19	2.1744
	15.0	4.71	1.2	2.7348
S-1	5.0	4.56	0.61	-2.4715
	7.5	4.65	0.82	-1.4884
	10.0	4.81	1.02	0.1980
	12.5	4.90	1.12	1.4166
	15.0	4.90	1.23	3.1052
S-2	5.0	3.45	0.81	-1.0536
	7.5	3.56	0.95	-0.3847
	10.0	3.71	1.1	0.9531
	12.5	3.71	1.2	2.2790
	15.0	4.12	1.27	3.5853
S-3	5.0	3.26	1.01	0.0498
	7.5	3.33	1.06	0.4370
	10.0	3.86	1.14	1.3103
	12.5	3.97	1.25	2.7893
	15.0	4.51	1.3	3.9355

present work, the Ozawa analysis is not discussed, as it is thought to be rather inapplicable.

Mo's Analysis

As the degree of crystallinity is found to be related to

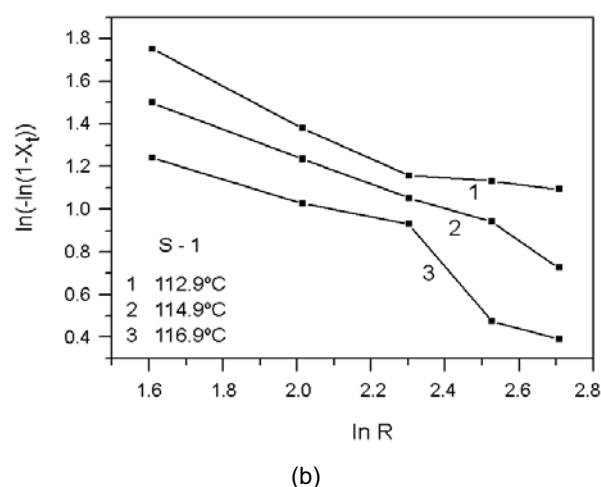
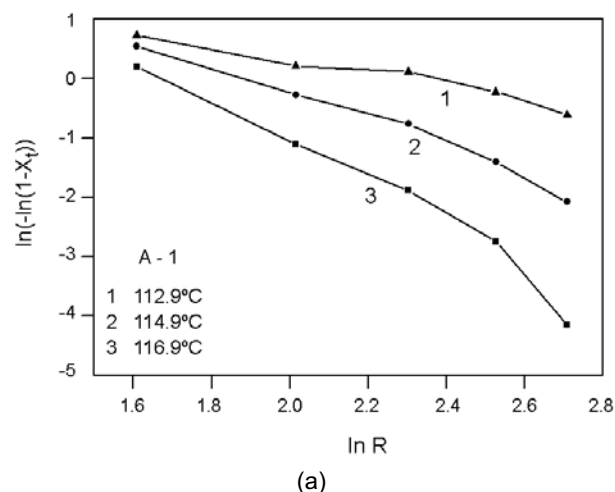
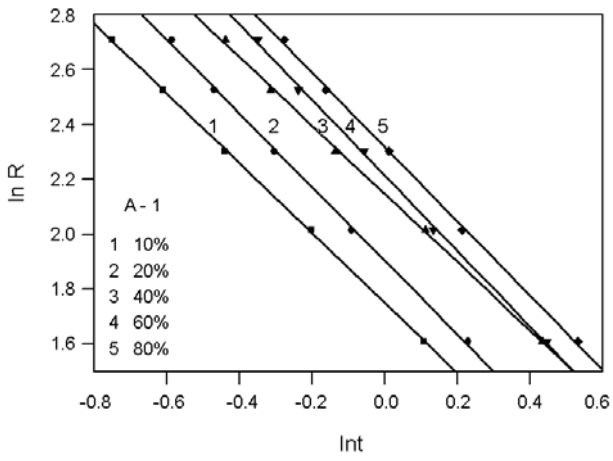


Figure 4. Ozawa plots of $\ln(-\ln(1-X_t))$ vs. $\ln R$ for crystallization of: (a) A-1 and (b) S-1 composites at different temperature.

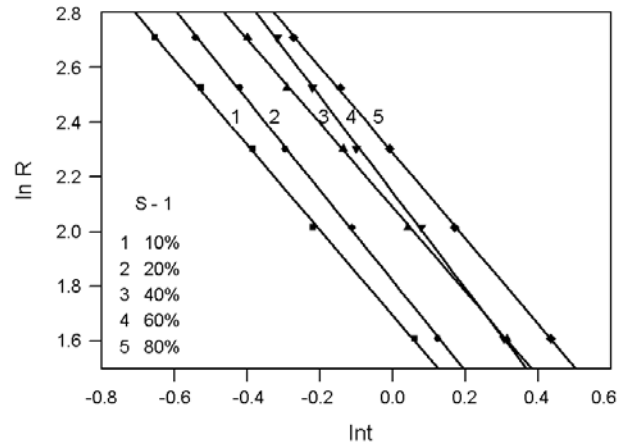
the cooling rate R and the crystallization time t (or temperature T), the relation between the cooling rate and the crystallization time for a given degree of crystallinity is defined by Mo, et al. [22] as follows:

$$\ln R = \ln F(T) - \alpha \ln t \tag{7}$$

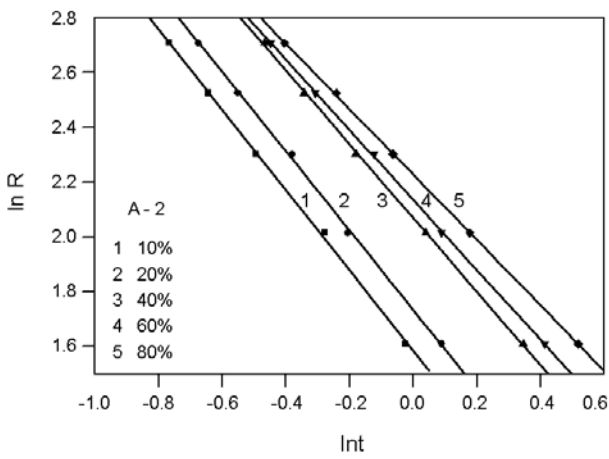
where, $F(T)$ refers to the value of cooling rate chosen at unit crystallization time when the system has a certain degree of crystallinity. The smaller the value of $F(T)$, the higher the crystallization rate would become. Therefore, $F(T)$ has a definite physical and practical meaning. The value of α is related to mechanism of nucleation. As shown in Figure 5, plotting $\ln R$ against $\ln t$, at a given relative degree of crystal-



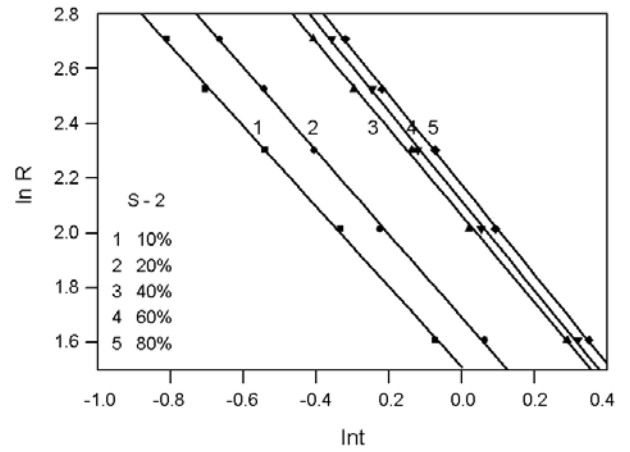
(a)



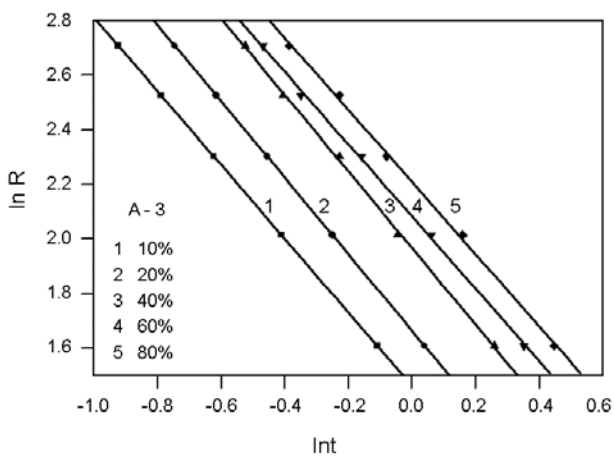
(d)



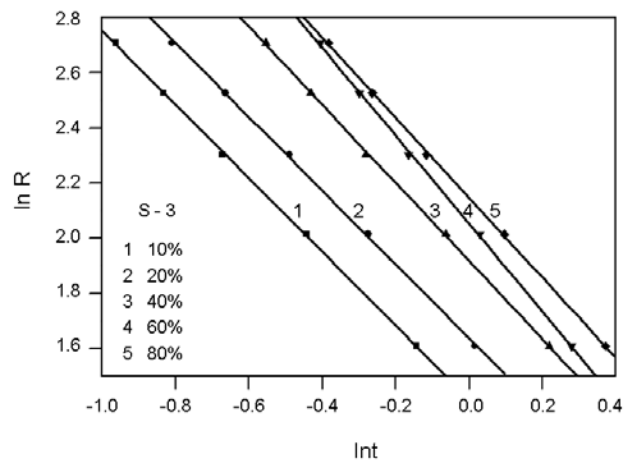
(b)



(e)



(c)



(f)

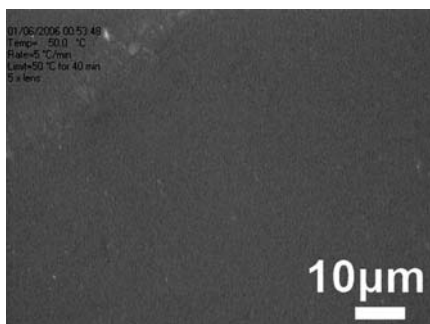
Figure 5. Mo plots of $\ln R$ vs. $\ln t$ for crystallization of: (a) A-1, (b) A-2, (c) A-3, (d) S-1, (e) S-2, and (f) S-3 composites.

Table 4. Non-isothermal crystallization kinetic parameters based on Mo's treatment.

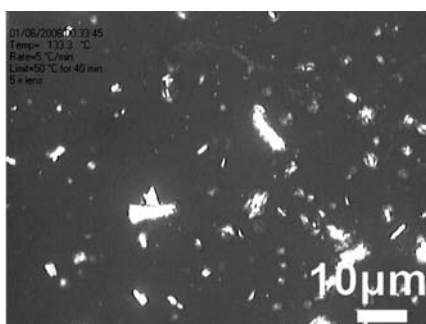
X_t (%)	iPP		A-1		A-2		A-3		S-1		S-2		S-3	
	F(T)	α	F(T)	α	F(T)	α	F(T)	α	F(T)	α	F(T)	α	F(T)	α
10	5.89	1.40	5.89	1.31	4.89	1.48	4.31	1.35	5.4	1.56	4.56	1.45	4.2	1.31
20	6.92	1.45	6.92	1.35	5.61	1.48	5.28	1.4	6.23	1.65	5.41	1.51	5.1	1.35
40	8.76	1.48	8.76	1.26	7.92	1.37	7.12	1.42	7.98	1.54	7.86	1.62	6.86	1.39
60	9.35	1.43	9.35	1.38	8.41	1.29	8.01	1.31	8.56	1.71	8.31	1.65	7.84	1.56
80	10.49	1.54	10.49	1.36	9.26	1.19	9.12	1.32	9.86	1.53	8.86	1.64	8.59	1.42

lization, a linear relationship is observed. The values of F(T) and the slope α are listed in Table 4 that shows the values of α are nearly the same for each sample. As the F(T) values increase with the relative degree of crystallinity within equal time intervals, a faster cooling rate R is required for the same sample to reach a higher degree of crystallinity which also means a larger F(T) value. Thus, when the crystallization time is the same, the relative degree of crystallinity would increase with the cooling rates.

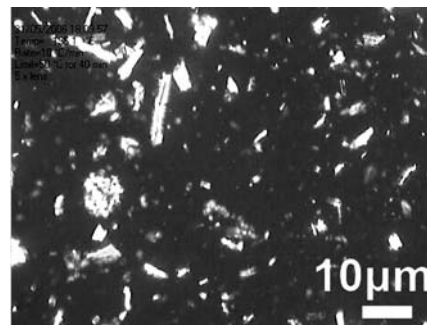
It can also be seen that F(T) systematically increases with the increasing the relative degree of crystallinity. It is also obvious that for a definite degree of crystallinity, F(T) for iPP/MCCs composites is smaller than that for iPP. This means that, to reach the same relative degree of crystallinity, iPP/MCCs composites require smaller cooling rates which indicate that iPP/MCCs composites crystallize at a faster rate than iPP. The higher the amount of MCC, the smaller would be the F(T) value. This indi-



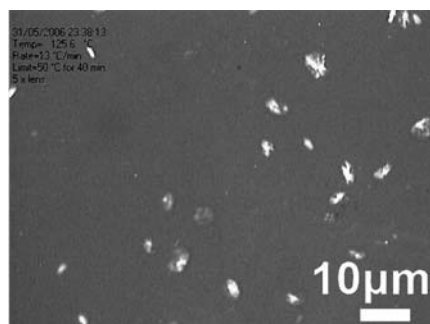
(a-5s)



(b-5s)



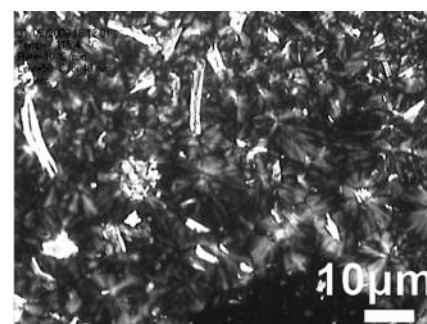
(c-5s)



(a-40s)



(b-40s)



(c-40s)

Continued

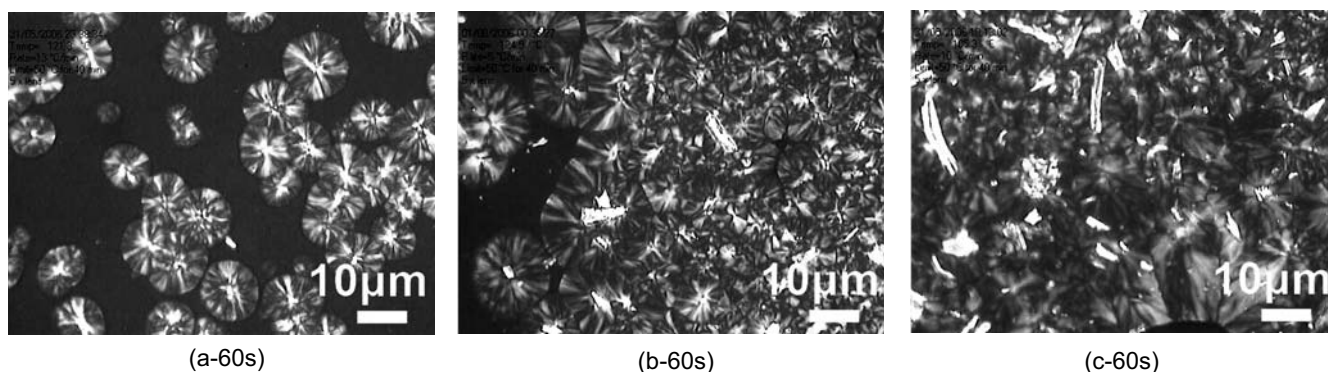


Figure 6. Polarized optical micrographs showing the morphology of crystals of: (a) PP, (b) PP/MCC1, and (c) PP/MCC2 composites at various time (magnification $\times 500$, crystallizing temperature 130°C).

cates that MCCs can raise the crystallization rate. On the other hand, the results show that at each relative degree of crystallinity, the value of $F(T)$ of iPP/MCC2 is lower than that of iPP/MCC1 which is in accordance with Jeziorny analysis; meaning that the heterogeneous nucleation effect of MCC2 must be stronger than that of MCC1.

Morphological Observations

Morphological observations were carried out by optical microscopy. Figure 6 shows the photographs of iPP/MCCs composites as well as that of pure iPP during isothermal crystallization process at 130°C . It is clear in Figure 6 that the nucleation rates of iPP/MCCs composites are larger than that of iPP, because of heterogeneous nucleation of MCCs particles. Induction periods of iPP, iPP/MCC1 (1%) and iPP/MCC2 (1%) are 15-40, 5-15, and <5 s, respectively.

Since, crystal growth is ultimately limited by facing spherulite boundary it will lead to an irregular final structure and smaller crystalline dimension. In Figure 6(5 s) a perfect spherulite shape is not evidently seen but, the intersections of Figure 6(60 s) clearly indicate the existence of a perfect spherulite [27-30]. The average spherulite sizes of iPP, iPP/MCC1, and iPP/MCC2 are about 35, 20 and $10\ \mu\text{m}$, respectively. Therefore, compared with others iPP/MCC2 has the least crystallization time and final crystal size at 130°C . It is well known that crystalline morphology significantly affects the mechanical properties of a material because a smaller crystal is prone to develop into a crack to absorb impact energy while a big spherulite is apt to form local

stress which makes the material brittle. Therefore, the crystalline morphology of iPP/MCC2 is favourable for its mechanical properties [31,32].

CONCLUSION

Three methods were used to deal with the non-isothermal crystallization process for iPP and iPP/MCCs composites. The Ozawa equation cannot satisfactorily describe the non-isothermal crystallization behaviour of iPP/MCCs composites, while Jeziorny's and Mo's methods can. According to the results obtained by Avrami equation, the primary crystallization stage for non-isothermal melt crystallization might correspond to a three-dimensional spherical growth with heterogeneous nucleation. The values of the rate parameter Z_c and the kinetics parameter $F(T)$ reveal that adding MCCs obviously increases the crystallization rate of iPP from molten state,. The results of DSC and polarized optical microscopy techniques indicate that MCC can increase the crystallization temperature and the nucleation density of iPP. Thus, MCC is an effective nucleating agent for iPP. When MCC1 or MCC2 are added to iPP, the crystallization rate increases and with the increasing amount of MCC the crystallization temperature, T_p increases as well.

ACKNOWLEDGEMENTS

The authors thank Donghua University for the provision of equipments, Mr Jianzhong Tang for technical

assistance, Dr. Biao Wang, Ms Jing Cui, Dr. Shuai ke Shi, and Dr. Zhiyong Yan for assistance in the use of equipment and for technical discussions.

REFERENCES

- Li Y, Fang QF, Yi ZG, Zheng K, A study of internal friction in polypropylene (PP) filled with nanometer-scale CaCO₃ particles, *Mater Sci Eng*, **A370**, 268-272, 2004.
- Seo MK, Lee JR, Park SJ, Crystallization kinetics and interfacial behaviors of polypropylene composites reinforced with multi-walled carbon nanotubes, *Mater Sci Eng*, **A404**, 79-84, 2005.
- George ZP, Dimitris SA, Dimitris NB, George PK, Crystallization kinetics and nucleation activity of filler in polypropylene/surface-treated SiO₂ nanocomposites, *Thermochim Acta*, **427**, 117-82, 2005.
- Luo BZ, Zhang J, Wang XL, Zhou Y, Wen JZ, Effects of nucleating agents and extractants on the structure of polypropylene microporous membranes via thermally induced phase separation, *Desalination*, **192**, 142-150, 2006.
- Shen H, Wang YH, Mai KC, Non-isothermal crystallization behavior of PP/Mg(OH)₂ composites modified by different compatibilizers, *Thermochim Acta*, **457**, 27-34, 2007.
- Ding C, Jia DM, He H, Guo BC, Hong HQ, How organo-montmorillonite truly affects the structure and properties of polypropylene, *Polym Test*, **24**, 94-100, 2005.
- Zhu G, Li CC, Li ZY, The effects of alkali dehydroabietate on the crystallization process of polypropylene, *Eur. Polym J*, **37**, 1007-1013, 2001.
- Gui QD, Xin Z, Zhu WP, Effect of an organic phosphorus nucleating agent on crystallization behaviors and mechanical properties of polypropylene, *J Appl Polym Sci*, **88**, 297-301, 2003.
- Hamad W, *Cellulosic Materials: Fibers, Networks and Composites*, Kluwer, Boston, p 47, 2002.
- Bledzki AK, Gassan J, Composites reinforced with cellulose based fibres, *Prog Polym Sci*, **24**, 221-74, 1999.
- Felix JM, Gatenholm P, The nature of adhesion in composites of modified cellulose fibers and polypropylene, *J Appl Polym Sci*, **42**, 609-20, 1991.
- Felix JM, Gatenholm P, Schreiber HP, Controlled interactions in cellulose-polymer composites. 1: Effect on mechanical properties, *Polym Compos*, **14**, 449-457, 1993.
- Sain MM, Kokta BV, Toughened thermoplastic composite. I. Cross-linkable phenol formaldehyde and epoxy resins-coated cellulosic-filled polypropylene composites, *J Appl Polym Sci*, **48**, 2181-2196, 1993.
- Collier JR, Lu M, Fahrurrozi M, Collier BJ, Cellulosic reinforcement in reactive composite systems, *J Appl Polym Sci*, **61**, 1423-1430, 1996.
- Amash A, Zugenmaier P, Study on cellulose and xylan filled polypropylene composites, *Polym bul*, **40**, 251-258, 1998.
- Eichhorn SJ, Baillie CA, Zafeiropoulos N, Mwaikambo LY, Ansell MP, Dufresne A, Entwistle KM, Herrera- Franco PJ, Escamilla GC, Groom L, Hughes M, Hill C, Rials TG, Wild PM, Current international research into cellulosic fibers and composites, *J Mater Sci*, **36**, 2107-2131, 2001.
- Endo T, Zhang F, Kitagawa R, Hirotsu T, Hosokawa J, Formation of hydrogen-bonds between particles of fine cellulose powder to yield a transparent cellulose plate, *J Polym*, **32**, 182-185, 2000.
- Avrami M, Kinetics of phase change. I. General theory, *J Chem Phys*, **7**, 1103-1112, 1939.
- Avrami M, Kinetics of phase change. II. Transformation-time relations for random distribution of nuclei, *J. Chem Phys*, **8**, 212-224, 1940.
- Jeziorny A, Parameters characterizing the kinetics of the nonisothermal crystallization of poly (ethylene terephthalate) determined by DSC, *Polymer*, **19**, 1142-1144, 1978.
- Ozawa T, A new method of analyzing thermogravimetric data, *Bull Chem Soc Jpn*, **38**, 1881-1886, 1965.
- Liu TX, Mo ZS, Wang S, Zhang HF, Nonisothermal melt and cold crystallization kinetics of poly (aryl ether ether ketone),

- Polym Eng Sci*, **37**, 568-575, 1997.
23. Addonizio ML, Martuscelli E, Silvestre C, Study of the nonisothermal crystallization of poly (ethylene oxide) /poly (methyl methacrylate) blends, *Polymer*, **28**, 183-188, 1987.
 24. Lopez LC, Wilkes GL, Nonisothermal crystallization kinetics of poly (p-phenylene sulfide), *Polymer*, **30**, 882-887, 1989.
 25. Di Lorenzo ML, Silvestre C, Non-isothermal crystallization of polymers, *Prog Polym Sci*, **24**, 917-950, 1999.
 26. Ziabicki A, Sajkiewicz P, Crystallization of polymers in variable external conditions. Part 3. Experimental determination of kinetic characteristics, *Colloid Polym Sci*, **276**, 680-689, 1998.
 27. Nowacki R, Monasse B, Piorkowska E, Galeski A, Haudin JM, Spherulite nucleation in isotactic polypropylene based nanocomposites with montmorillonite under shear, *Polymer*, **45**, 4877-4892, 2004.
 28. Zhang JL, Liu ZM, Han BX, Jiang T, Wu WZ, Chen J, Li ZH, Liu DX, Preparation of Polystyrene-Encapsulated Silver Nanorods and Nanofibers by Combination of Reverse Micelles, Gas Antisolvent, and Ultrasound Techniques, *J Phys Chem B*, **108**, 2200-2204, 2004.
 29. Ryu JG, Park SW, Kim H, Lee JW, Power ultrasound effects for in situ compatibilization of polymer-clay nanocomposites, *Mater Sci Eng C*, **24**, 285-288, 2004.
 30. Artzi N, Nir Y, Narkis M, Siegmann A, Melt blending of ethylene-vinyl alcohol copolymer/clay nanocomposites: effect of the clay type and processing conditions, *J Polym Sci Polym Phys*, **40**, 1741-1753, 2002.
 31. Lee EC, Mielewski DF, Baird RJ, Exfoliation and dispersion enhancement in polypropylene nanocomposites by in-situ melt phase ultrasonication, *Polym Eng Sci*, **44**, 1773-1782, 2004.
 32. Li J, Zhao LJ, Guo SY, Ultrasonic preparation of polymer/layered silicate nanocomposites during extrusion, *Polym Bull*, **55**, 217-223, 2005.